ARTICLE

¹Hᴺ, ¹³C, and ¹⁵N resonance assignments of the *Clostridioides difficile* receptor binding domain 2 (CDTb, residues 757–876)

Mary E. Cook[1] · Kristen M. Varney[1] · Raquel Godoy-Ruiz[1] · David J. Weber[1]

Abstract

Clostridioides difficile is a bacterial pathogen responsible for the majority of nosocomial infections in the developed world. *C. difficile* infection (CDI) is difficult to treat in many cases because hypervirulent strains have evolved that contain a third toxin, termed the *C. difficile* toxin (CDT), in addition to the two enterotoxins TcdA and TcdB. CDT is a binary toxin comprised of an enzymatic, ADP-ribosyltransferase (ART) toxin component, CDTa, and a pore-forming or delivery subunit, CDTb. In the absence of CDTa, CDTb assembles into two distinct di-heptameric states, a symmetric and an asymmetric form with both states having two surface-accessible host cell receptor-binding domains, termed RBD1 and RBD2. RBD1 has a unique amino acid sequence, when aligned to other well-studied binary toxins (i.e., anthrax), and it contains a novel Ca²⁺-binding site important for CDTb stability. The other receptor binding domain, RBD2, is critically important for CDT toxicity, and a domain such as this is missing altogether in other binary toxins and shows further that CDT is unique when compared to other binary toxins. In this study, the ¹H, ¹³C, and ¹⁵N backbone and sidechain resonances of the 120 amino acid RBD2 domain of CDTb (residues 757–876) were assigned sequence-specifically and provide a framework for future NMR-based drug discovery studies directed towards targeting the most virulent strains of CDI.

Keywords *Clostridioides difficile* · CDI · CDTb · Binary toxin

Biological context

Clostridioides difficile infection (CDI) is caused by a spore-forming, Gram-positive bacterium, and it is the most commonly reported nosocomial infection in the world, accounting for 12% of all hospital-borne infections (Gerding 2015). Prior to the emergence of hypervirulent strains early in the twenty-first century, *C. difficile* strains produced only two large enterotoxins, TcdA and TcdB, which inhibit signaling pathways by glucosylating small GTPases. Whereas, hypervirulent strains emerging more recently, such as the NAP1 epidemic strain, encode TcdA/TcdB plus additional virulence factors, most notably a third toxin termed the *C. difficile* toxin (CDT) (Perelle et al. 1997). CDT is a binary toxin that kills host cells by covalent modification of

essential intracellular regulators of host cell function, including G-actin. While drug options are becoming available to target the large clostridial toxins in CDI, TcdA/TcdB (Yang et al. 2015), there is nothing approved by the FDA to target CDT (Secore et al. 2017). To address this unmet medical need, potent and selective CDT inhibitors are needed to provide treatment option(s) for patients infected with the most serious hypervirulent CDT-containing strains of CDI.

CDT has an enzymatic subunit, CDTa (47.4 kDa), with ribosyltransferase activity, and a pore-forming delivery subunit, termed CDTb (74 kDa). Fully active CDT associates in a 1:7 ratio of CDTa to CDTb subunits (Goorhuis et al. 2008; Loo et al. 2005; McDonald et al. 2005; Rupnik 2008; Stewart et al. 2013; Geric et al. 2004). Prior to cellular entry via endosomes (Hale et al. 2004; Nagahama et al. 2000, 2004; Gibert et al. 2011), the binary toxin complex associates with membrane-bound host cell receptor(s), such as the lipolysis-stimulated lipoprotein receptor (LSR) and/or CD44 (Wigelsworth et al. 2012; Papatheodorou et al. 2011; Fagan-Solis et al. 2014; Hiramatsu et al. 2017). CDT enters the host cell via endosomes with the low pH in endosomes triggering CDTa translocation into

✉ David J. Weber
  dweber@som.umaryland.edu

[1] Department of Biochemistry and Molecular Biology, Center for Biomolecular Therapeutics (CBT), University of Maryland School of Medicine, 108 N. Greene St., Baltimore, MD 21201, USA

the cytoplasm via the pore-forming entity, CDTb (Bachmeyer et al. 2001; Blocker et al. 2003; Haug et al. 2003; Knapp et al. 2002; Krantz et al. 2004, 2005, 2006; Lang et al. 2008; Schmid et al. 1994; Knapp et al. 2016). Upon delivery of the catalytically active CDTa enzyme into the host cell cytoplasm, ADP-ribosylation of G-actin occurs rapidly at Arg177 (Sundriyal et al. 2009). Modified G-actin leads to F-actin filament dissociation (Gulke et al. 2001), destruction of the cytoskeleton, increased microtubule protrusions, accelerated bacterial adhesion, and a "*death spiral*" for mammalian host cells (Gerding et al. 2014; Benz 2017; Barth 2017). Of interest here is the host-cell binding component of CDT, CDTb. Recent structural studies of CDTb showed that it exists in two states, either as an asymmetric or a symmetric di-heptamer, in the absence of CDTa (Gerding et al. 2014; Xu et al. 2020). The asymmetric form, [Asym]CDTb, has one of its two heptameric components folding into a seven-stranded beta-barrel with an internal cavity that is reminiscent of the anthrax protective antigen (PA) (Akkaladevi et al. 2013). Although, when compared to other binary toxins, CDTb was found to have two distinct host cell receptor-binding domains, RBD1 and RBD2, rather than just a single domain. In addition, RBD1 lacks sequence homology to any other known toxin and contains a novel calcium-binding site needed for protein stability (Xu et al. 2020). Whereas, the RBD2 domain is absent altogether in other well-studied binary toxins, including anthrax. Importantly, RBD2 was shown to provide a potent dominant negative effect for host cell toxicity when isolated (residues 757–876) indicating its important functional role within hypervirulent CDI (Xu et al. 2020). Therefore, with these data in hand, the sequence-specific backbone and sidechain resonance assignments of RBD2 were completed as a first step towards designing RBD2 inhibitors using NMR-based methods, which will be important for the longer-term goal of targeting toxicities associated with hypervirulent *Clostridioides difficile* that produces CDT.

Methods and experiments

Protein expression and purification

As previously described (Xu et al. 2020), DNA encoding the RBD2 binding domain of CDTb (residues 757–876) was codon optimized and engineered into pET21 expression plasmid along with a His-tag at its N-terminus, as was needed for solubility and purification purposes (TOPGene Technologies). The RBD2-containing expression plasmid was transformed into the *E. coli* BLR(DE3) cells, and large-scale protein over-production was performed using 2 L of defined [^{15}N, ^{13}C]-labeled MOPS media, containing 1 g/L of ^{15}N-labeled NH4Cl and 2.5 g/L of ^{13}C-labeled D-Glucose

per liter of media. IPTG (0.5 mM) was added to the media when the A_{600} cell density reading was between 0.7 and 0.8 O.D., at which time the cells were grown for an additional 18 h at 25 °C. At the end of the growth period, the cells were centrifuged for 15 min at 4000 r.p.m, and the pellets were weighed and resuspended in a lysis buffer containing 50 mM Tris–HCl, pH 8.0, 500 mM NaCl, 10 mM BME such that 3 mL of lysis buffer were added per gram of wet pellet. Prior to sonication, the cell lysate was incubated at 4 °C for 1 h with DNase, 10 mM $CaCl_2$ and 10 mM $MgCl_2$. Three cycles of sonication at 50% power amplitude were performed next and followed by centrifugation at 15,000 r.p.m for 45 min at 4 °C to remove cell debris. The clear supernatant was filtered and loaded onto a previously equilibrated HiPrep 16/60 IMAC column with buffer A (20 mM Tris–HCl, pH 8.0, 300 mM NaCl, 10 mM BME). Upon addition of buffer B (buffer A plus 1 M imidazole) to the column, the RBD2 construct was eluted at ~ 150 mM imidazole into 5 mL fractions and analyzed by SDS-PAGE. The RBD2-containing fractions were pooled, concentrated, and injected onto a Superdex S200-PG size exclusion column previously equilibrated with 15 mM HEPES buffer, pH 7.0, 150 mM NaCl, and 0.5 mM DTT. Fractions containing the RBD2 construct were eluted from the S200 column and shown to be pure via SDS- and native-PAGE (> 99%). The yield of the RBD2 domain was typically > 50 mg of purified protein per liter of bacterial cell culture, and its concentration was adjusted to ~ 1 mM, aliquoted, and stored at − 80 °C, prior to preparing NMR samples.

NMR spectroscopy

NMR data was collected at 25 °C on Bruker 950 MHz, 800 MHz, and 600 MHz spectrometers. The NMR samples all contained 0.5 mM of the RBD2 domain, 15 mM HEPES buffer, pH 7.0, and 150 mM NaCl in 90% H_2O and 10% D_2O. The NMR sample was of high-quality as judged by a 2D ^{1}H,^{15}N-edited HSQC spectrum shown together with sequence-specific resonance assignments (Fig. 1a). The observable backbone and sidechain ^{1}H, ^{13}C, and ^{15}N resonances were assigned via pairwise comparison of inter- and intra-residue ^{13}Cα, ^{13}Cβ and ^{13}C′ chemical shift values from 3D HNCA, HN(CO)CA, HNCACB – CB optimized, CACB(CO)NH, HC(CO)NH, C(CO)NH, and HNCO experiments (Grzesiek 1992; Kay et al. 1994; Wittekind 1993; Montelione et al. 1992). The NMR data were processed with NMRPipe and analyzed using CcpNMR software (Delaglio et al. 1995; Vranken et al. 2005), and the secondary structure prediction was achieved using a Chemical Shift Index (CSI) algorithm on the CSI 2.0 web server (Berjanskii 2005). All proton chemical shifts were referenced to external trimethylsilyl propanoic acid (TSP) at 25 °C (0.00 ppm) with respect to residual H_2O (4.698 ppm). The ^{15}N and ^{13}C chemical shift
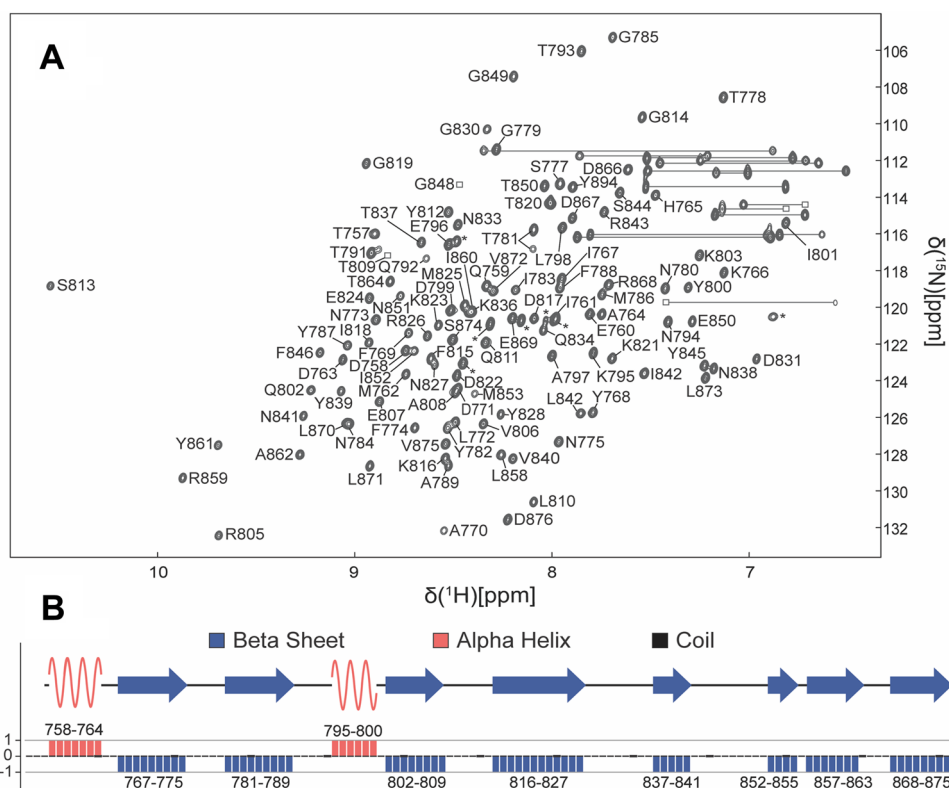
Fig. 1 Resonance assignments and secondary structure of the receptor binding domain 2 (RBD2) domain of CDTb. **a** The 2D ^{1}H,^{15}N-edited HSQC spectrum of RBD2 (residues 757–876) recorded on a Bruker 950 MHz spectrometer at pH 7.0 and 25 °C. Residue type and number indicate assignments from backbone amide H^{N} correlations. Horizontal lines are illustrated for ^{1}H-^{15}N correlations arising from sidechain asparagine (Asn) and glutamine (Gln) residues, and correlations labeled with an asterisk (*) arise from residues within the His-tag region of the RBD2 construct. **b** The secondary structure of RBD2 predicted from the chemical shift index method is illustrated and consists of 8 beta strands (β1, I767-N775; β2, T781-A789; β3, Q802-T809; β4, K816-N827; β5, T837-N841; β6, I852-Y855; β7, K857-I863; β8, R868-V875) shown with blue arrows and 2 alpha helices (α1, D758-A764; α2, K795-Y800) highlighted in red. The remaining regions of RBD2 are predicted to exist as random coil and are shown with a black line in the secondary structure representation

values reported were indirectly referenced using zero-point frequency ratios of 0.101329118 and 0.251449530, respectively (Wishart et al. 1995).

Extent of assignment and data deposition

Sequence-specific resonance assignments shown in Fig. 1a were determined unambiguously using heteronuclear multidimensional NMR methods for 110 out of the 115 possible H^{N}–^{15}N correlations (~96%) of the receptor-binding domain-2 (RBD2) of CDTb. Of those 110 correlations, 100% of the CA, 95% of the CB, and 94% of the CO chemical shifts were determined. It was also possible to assign 7 of the 12 residues in the His-tag, which are labeled with an asterisk (*) in Fig. 1. The 120-residue RBD2 domain has five proline residues (Pro776, Pro790, Pro832, Pro835, and Pro865) that do not provide ^{1}H–^{H}N correlations. Four of the other five residues that do not appear in the 2D ^{1}H,^{15}N-edited HSQC spectrum reside in a small stretch of sequence in the C-terminal region of RBD2 (Thr854, Tyr855, Lys856,

Lys857), and the fifth missing correlation was for residue Leu829. It is likely that non-proline missing correlations were the result of conformational averaging occurring on the chemical shift timescale. Two residues, Thr781 and Ileu783, were each found to have two H$_{N}$ correlations having different ^{1}H and ^{15}N chemical shift values with varying intensities (~80:20), but the chemical shift values for their respective pairs of inter- and intra-residue carbon correlations to carbon (i.e. HNCA, HNCACB, etc.) were identical. While it is possible that peak doubling such as this could arise from a cis-trans proline isomerization, on the slow chemical shift timescale, a more likely explanation is that the sidechain of Tyr782 has two slowly exchanging conformational states. Nonetheless, providing a foolproof conclusion to this question of doubling is beyond the scope of this assignment note, and requires additional experimentation that will be reported elsewhere. The chemical shift values assigned for RBD2 were used next as input for a chemical shift index (CSI) algorithm to map the secondary structure of RBD2. As shown in Fig. 1b, the secondary structure from

CSI analyses predicts that the RBD domain has eight beta strands (I767-N775; T781-A789; Q802-T809; K816-N827; T837-N841; I852-Y855; K857-I863; R868-V875) and 2 alpha helices (D758-A764; K795-Y800), which is fully consistent with the X-ray and cryoEM structures reported previously (Xu et al. 2020). In summary, the chemical shift values for backbone and sidechain resonances of RBD2 obtained here were deposited in the Biological Magnetic Resonance Bank database (http://www.bmrb.wisc.edu) under accession number 28,131, and these data will be important for next-stage NMR studies that map RBD2 biomolecular interactions and for developing inhibitors targeting CDTb.

Compliance with Ethical Standards

References

Akkaladevi N, Hinton-Chollet L, Katayama H, Mitchell J, Szerszen L, Mukherjee S, Gogol EP, Pentelute BL, Collier RJ, Fisher MT (2013) Assembly of anthrax toxin pore: lethal-factor complexes into lipid nanodiscs. Protein Sci 22:492–501

Bachmeyer C, Benz R, Barth H, Aktories K, Gilbert M, Popoff MR (2001) Interaction of *Clostridium botulinum* C2 toxin with lipid bilayer membranes and Vero cells: inhibition of channel function by chloroquine and related compounds in vitro and in toxification in vivo. FASEB J 15:1658–1660

Barth H (2017) An introduction to the toxins special issue on "Novel pharmacological inhibitors for bacterial protein toxins." Toxins (Basel) 9(5):160

Benz R, Barth H (2017) Toxin transport by A-B type of toxins in eukaryotic target cells and its inhibition by positively charged heterocyclic molecules. Curr Top Microbiol Immunol 406:229–256

Berjanskii MV, Wishart DS (2005) A simple method to predict protein flexibility using secondary chemical shifts. J Am Chem Soc 127:14970–14971

Blocker D, Bachmeyer C, Benz R, Aktories K, Barth H (2003) Channel formation by the binding component of *Clostridium botulinum* C2 toxin: glutamate 307 of C2II affects channel properties in vitro and pH-dependent C2I translocation in vivo. Biochemistry 42:5368–5377

Delaglio F, Grzesiek S, Vuister GW, Zhu G, Pfeifer J, Bax A (1995) NMRPipe: a multidimensional spectral processing system based on UNIX pipes. J Biomol NMR 6:277–293

Fagan-Solis KD, Reaves DK, Rangel MC, Popoff MR, Stiles BG, Fleming JM (2014) Challenging the roles of CD44 and lipolysis stimulated lipoprotein receptor in conveying *Clostridium perfringens* iota toxin cytotoxicity in breast cancer. Mol Cancer 13:163

Gerding DN, Johnson S, Rupnik M, Aktories K (2014) *Clostridium difficile* binary toxin CDT: mechanism, epidemiology, and potential clinical importance. Gut Mcrobes 5:15–27

Gerding DN, Lessa FC (2015) The epidemiology of *Clostridium difficile* infection inside and outside health care institutions. Infect Dis Clin N Am 29:37–50

Geric B, Rupnik M, Gerding DN, Grabnar M, Johnson S (2004) Distribution of *Clostridium difficile* variant toxinotypes and strains with binary toxin genes among clinical isolates in an American hospital. J Med Microbiol 53:887–894

Gibert M, Monier MN, Ruez R, Hale ML, Stiles BG, Benmerah A, Johannes L, Lamaze C, Popoff MR (2011) Endocytosis and toxicity of clostridial binary toxins depend on a clathrin-independent pathway regulated by Rho-GDI. Cell Microbiol 13:154–170

Goorhuis A, Bakker D, Corver J, Debast SB, Harmanus C, Notermans DW, Bergwerff AA, Dekker FW, Kuijper EJ (2008) Emergence of *Clostridium difficile* infection due to a new hypervirulent strain, polymerase chain reaction ribotype 078. Clin Infect Dis 47:1162–1170

Grzesiek S, Bax A (1992) An efficient experiment for sequential backbone assignment of medium-sized isotopically enriched proteins. J Magn Reson 99:201–207

Gulke I, Pfeifer G, Liese J, Fritz M, Hofmann F, Aktories K, Barth H (2001) Characterization of the enzymatic component of the ADP-ribosyltransferase toxin CDTa from *Clostridium difficile*. Infect Immun 69:6004–6011

Hale ML, Marvaud JC, Popoff MR, Stiles BG (2004) Detergent-resistant membrane microdomains facilitate Ib oligomer formation and biological activity of *Clostridium perfringens* iota-toxin. Infect Immun 72:2186–2193

Haug G, Wilde C, Leemhuis J, Meyer DK, Aktories K, Barth H (2003) Cellular uptake of *Clostridium botulinum* C2 toxin: membrane translocation of a fusion toxin requires unfolding of its dihydrofolate reductase domain. Biochemistry 42:15284–15291

Hiramatsu K, Serada S, Enomoto T, Takahashi Y, Nakagawa S, Nojima S, Morimoto A, Matsuzaki S, Yokoyama T, Takahashi T, Fujimoto M, Takemori H, Ueda Y, Yoshino K, Morii E, Kimura T, Naka T (2017) LSR antibody therapy inhibits ovarian epithelial tumor growth by inhibiting lipid uptake. Cancer Res 78(2):516–527

Kay LE, Xu GY, Tamazaki T (1994) Enhanced-sensitivity triple-resonance spectroscopy with minimal H2O saturation. J Magn Reson A109:129–133

Knapp O, Benz R, Gibert M, Marvaud JC, Popoff MR (2002) Interaction of *Clostridium perfringens* iota-toxin with lipid bilayer membranes. Demonstration of channel formation by the activated binding component Ib and channel block by the enzyme component Ia. J Biol Chem 277:6143–6152

Knapp O, Benz R, Popoff MR (2016) Pore-forming activity of clostridial binary toxins. Biochim Biophys Acta 1858:512–525

Krantz BA, Trivedi AD, Cunningham K, Christensen KA, Collier RJ (2004) Acid-induced unfolding of the amino-terminal domains of the lethal and edema factors of anthrax toxin. J Mol Biol 344:739–756

Krantz BA, Melnyk RA, Zhang S, Juris SJ, Lacy DB, Wu Z, Finkelstein A, Collier RJ (2005) A phenylalanine clamp catalyzes protein translocation through the anthrax toxin pore. Science 309:777–781

Krantz BA, Finkelstein A, Collier RJ (2006) Protein translocation through the anthrax toxin transmembrane pore is driven by a proton gradient. J Mol Biol 355:968–979

Lang AE, Neumeyer T, Sun J, Collier RJ, Benz R, Aktories K (2008) Amino acid residues involved in membrane insertion and pore formation of *Clostridium botulinum* C2 toxin. Biochemistry 47:8406–8413

Loo VG, Poirier L, Miller MA, Oughton M, Libman MD, Michaud S, Bourgault AM, Nguyen T, Frenette C, Kelly M, Vibien A, Brassard P, Fenn S, Dewar K, Hudson TJ, Horn R, Rene P, Monczak Y, Dascal A (2005) A predominantly clonal multi-institutional outbreak of *Clostridium difficile*-associated diarrhea with high morbidity and mortality. N Engl J Med 353:2442–2449

McDonald LC, Killgore GE, Thompson A, Owens RC Jr, Kazakova SV, Sambol SP, Johnson S, Gerding DN (2005) An epidemic, toxin gene-variant strain of *Clostridium difficile*. N Engl J Med 353:2433–2441

Montelione GT, Lyons BA, Emerson SD, Tashiro M (1992) An efficient triple resonance experiment using carbon-13 isotropic mixing for determining sequence-specific resonance assignments of isotopically-enriched proteins. J Am Chem Soc 114:10974–10975

Nagahama M, Sakaguchi Y, Kobayashi K, Ochi S, Sakurai J (2000) Characterization of the enzymatic component of *Clostridium perfringens* iota-toxin. J Bacteriol 182:2096–2103

Nagahama M, Yamaguchi A, Hagiyama T, Ohkubo N, Kobayashi K, Sakurai J (2004) Binding and internalization of *Clostridium perfringens* iota-toxin in lipid rafts. Infect Immun 72:3267–3275

Papatheodorou P, Carette JE, Bell GW, Schwan C, Guttenberg G, Brummelkamp TR, Aktories K (2011) Lipolysis-stimulated lipoprotein receptor (LSR) is the host receptor for the binary toxin *Clostridium difficile* transferase (CDT). Proc Natl Acad Sci USA 108:16422–16427

Perelle S, Gibert M, Bourlioux P, Corthier G, Popoff MR (1997) Production of a complete binary toxin (actin-specific ADP-ribosyltransferase) by *Clostridium difficile* CD196. Infect Immun 65:1402–1407

Rupnik M (2008) Heterogeneity of large clostridial toxins: importance of *Clostridium difficile* toxinotypes. FEMS Microbiol Rev 32:541–555

Schmid A, Benz R, Just I, Aktories K (1994) Interaction of *Clostridium botulinum* C2 toxin with lipid bilayer membranes. Formation of cation-selective channels and inhibition of channel function by chloroquine. J Biol Chem 269:16706–16711

Secore S, Wang S, Doughtry J, Xie J, Miezeiewski M, Rustandi RR, Horton M, Xoconostle R, Wang B, Lancaster C, Kristopeit A, Wang SC, Christanti S, Vitelli S, Gentile MP, Goerke A, Skinner J, Strable E, Thiriot DS, Bodmer JL, Heinrichs JH (2017) Development of a novel vaccine containing binary toxin for the prevention of *Clostridium difficile* disease with enhanced efficacy against NAP1 strains. PLoS ONE 12:e0170640

Stewart DB, Berg A, Hegarty J (2013) Predicting recurrence of *C. difficile* colitis using bacterial virulence factors: binary toxin is the key. J Gastrointest Surg 17:118–125

Sundriyal A, Roberts AK, Shone CC, Acharya KR (2009) Structural basis for substrate recognition in the enzymatic component of ADP-ribosyltransferase toxin CDTa from *Clostridium difficile*. J Biol Chem 284:28713–28719

Vranken WF, Boucher W, Stevens TJ, Fogh RH, Pajon A, Llinas M, Ulrich EL, Markley JL, Ionides J, Laue ED (2005) The CCPN data model for NMR spectroscopy: development of a software pipeline. Proteins 59:687–696

Wigelsworth DJ, Ruthel G, Schnell L, Herrlich P, Blonder J, Veenstra TD, Carman RJ, Wilkins TD, Van Nhieu GT, Pauillac S, Gibert M, Sauvonnet N, Stiles BG, Popoff MR, Barth H (2012) CD44 promotes intoxication by the clostridial iota-family toxins. PLoS ONE 7:e51356

Wishart DS, Bigam CG, Yao J, Abildgaard F, Dyson HJ, Oldfield E, Markley JL, Sykes BD (1995) ^{1}H, ^{13}C, and ^{15}N resonance chemical shift referencing in biomolecular NMR. J Biomol NMR 6:135–140

Wittekind M, Mueller L (1993) HNCACB, a high-sensitivity 3D NMR experiment to correlate amide-proton and nitrogen resonances with the alpha- and beta-carbon resonances in proteins. J Magn Reson B 101:201–205

Xu X, Godoy-Ruiz R, Adipietro KA, Peralta C, Ben-Hail D, Varney KM, Cook ME, Roth BM, Wilder PT, Cleveland T, Grishaev A, Neu HM, Michel SLJ, Yu W, Beckett D, Rustandi RR, Lancaster C, Loughney JW, Kristopeit A, Christanti S, Olson JW, MacKerell AD, Georges AD, Pozharski E, Weber DJ (2020) Structure of the cell-binding component of the *Clostridium difficile* binary toxin reveals a di-heptamer macromolecular assembly. Proc Natl Acad Sci USA 117:1049–1058

Yang Z, Ramsey J, Hamza T, Zhang Y, Li S, Yfantis HG, Lee D, Hernandez LD, Seghezzi W, Furneisen JM, Davis NM, Therien AG, Feng H (2015) Mechanisms of protection against *Clostridium difficile* infection by the monoclonal antitoxin antibodies actoxumab and bezlotoxumab. Infect Immun 83:822–831